Materials Sciences and Applications, **2011, 2, 1180-1187**
doi:10.4236/msa.2011.29159 Published Online September 2011 (http://www.SciRP.org/journal/msa)

On the Electrical and Thermal Conductivities of Cast A356/Al_2O_3 Metal Matrix Nanocomposites

El-Sayed Youssef El-Kady, Tamer Samir Mahmoud, Ali Abdel-Aziz Ali

Mechanical Engineering Department, Faculty of Engineering, King Khalid University (KKU), Abha, Kingdom of Saudi Arabia.
Email: Eyelkady@yahoo.com

Received May 13th, 2011; revised June 2nd, 2011; accepted June 7th, 2011.

ABSTRACT

To assess the effect of the dispersion of Al_2O_3 nanoparticles into A356 Al alloy on both the electrical and thermal conductivities, A356/Al_2O_3 metal matrix nanocomposites (MMNCs) were fabricated using a combination of rheocasting and squeeze casting techniques. Two different sizes of Al_2O_3 nanoparticles were dispersed into the A356 Al alloy, typically, 60 and 200 nm with volume fractions up to 5 vol%. The effect of the nanoparticles size and volume fraction on the electrical and thermal conductivities was evaluated. The results revealed that the A356 monolithic alloy exhibited better electrical and thermal conductivities than the MMNCs. Increasing the nanoparticles size and/or the volume fraction reduces both the thermal and electrical conductivities of the MMNCs. The maximum reduction percent in the thermal and electrical conductivities, according to the A356 monolithic alloy, were about 47% and 38%, respectively. Such percentages were exhibited by A356/Al_2O_3 MMNCs containing 5 vol% of nanoparticles having 60 and 200 nm, respectively.

Keywords*: *Nanocomposites*, *Thermal Conductivity*, *Electrical Conductivity*, *Aluminum Alloys

1. Introduction

Metal matrix nanocomposites (MMNCs) reinforced by nanoscale particulates is one type of nanocomposite. MMNCs reinforced with nanoparticles are widely used in industry. Several applications of Al and Mg MMNCs are found in automotive and aerospace industry [1,2].

Conventional particulate reinforced metal matrix composites (MMCs) usually have a metallic phase (usually Al or Mg) and a ceramic reinforcement phase (most commonly SiC, Al_2O_3 and graphite particulates) composed of micron scale particles. Ingot metallurgy (I/M) (or casting techniques) and powder metallurgy (P/M) are common methods to produce conventional MMCs [2]. MMCs have higher yield strength, stiffness and lower coefficient of thermal expansion than those of the monolithic matrix alloy. Currently, there are several fabrication methods of MMNCs, including mechanical alloying, powder metallurgy, casting techniques, electrochemical deposition, friction stir processing, laser and sol-gel technology [1]. Each of these methods has its own advantages and disadvantages. Mechanical alloying, powered metallurgy and casting technique are the most commonly used techniques for producing bulk MMNCs [3]. With electrochemical deposition, laser technology and sol-gel fabrication methods, only thin films or layer of nanostructured MMNCs are formed.

The rheocasting (compocasting), as a semi-solid phase process, can produce good quality MMCs [4,5]. The technique has several advantages: It can be performed at temperatures lower than those conventionally employed in foundry practice during pouring; resulting in reduced thermochemical degradation of the reinforced surface, the material exhibits thixotropic behaviour typical of stir-cast alloys, and production can be carried out using conventional foundry methods. The preparation procedure for rheocast composites consists of the incorporation of the ceramic particles within very vigorously agitated semi-solid alloy slurry which can achieve more homogenous particles distribution as compared with a fully molten alloy. This is because of the presence of the solid phase in the viscous slurry that prevents the ceramic particles from settling and agglomerating. However, the composites produced by rheocasting suffer from the high porosity content, which has a deleterious effect on the mechanical properties. It has been reported that the porosity can be reduced by means of mechanical working such as extrusion or rolling on the solidified composites

or by applying a pressure to the composite slurry during solidification [6,7].

However the mechanical and tribological characteristics of MMNCs were extensively studied [8,9], only limited data on the thermal and electrical behavior of such nanocomposites are available [10,11]. Until now the thermal and electrical behaviour of MMNCs were not sufficiently determined and published. Accordingly, the aim of the present work is to study the effect of the Al_2O_3 nanoparticles additives on both the electrical and the thermal conductivities of A356 Al alloy. The effect of the Al_2O_3 nanoparticles size and volume fraction of the aforementioned conductivities was evaluated. The A356/Al_2O_3 MMNCs were fabricated a combination of rheocasting and squeeze casting techniques.

2. Experimental Procedures

The A356 Al-Si-Mg cast alloy was used as a matrix. The chemical composition of the A356 Al alloy is listed in **Table 1**. Nano-Al_2O_3 particulates were used as reinforcing agents. The Al_2O_3 nanoparticles have two different average sizes, typically, 200 and 60 nm. Several A356/Al_2O_3 MMNCs were fabricated with different volume factions of nanoparticles up to 5 vol%.

The A356/Al_2O_3 MMNCs were prepared using a combination of rheocasting and squeeze casting techniques. Preparation of the composite alloy was carried out according to the following procedures: About 1 kg of the A356 Al alloy was melted at 680˚C in a graphite crucible in an electrical resistance furnace. After complete melting and degassing by argon gas of the alloy, the alloy was allowed to cool to the semisolid temperature of 602˚C. At such temperature the liquid/solid fraction was about 0.7. The liquid/solid ratio was determined using primary differential scanning calorimeter (DSC) experiments performed on the A356 alloy. A simple mechanical stirrer with three blades made from stainless steel coated with bentonite clay was introduced into the melt and stirring was started at approximately 1000 rpm. Before stirring the nano-particles reinforcements after heating to 400˚C for two hours were added inside the vortex formed due to stirring. After that, preheated Al_2O_3 nanoparticles were introduced into the matrix during the agitation. After completing the addition of Al_2O_3 nanoparticles, the agitation was stopped and the molten mixture was poured into preheated tool steel mould and immediately squeezed during solidification using a hydraulic press of 50 ton capacity for 5 minutes.

Table 1. The chemical composition (wt%) of the A356 alloy.

Si	Fe	Cu	Mn	Mg	Zn	Al
6.6	0.25	0.11	0.002	0.14	0.026	Bal.

The MMNCs were heat treated at T6 before testing. The MMNCs were solution treated at 540˚C ± 1˚C for three hours and then quenched in cold water. After cooling specimens were artificially aged at 160˚C ± 1˚C for 12 hours.

Samples from the fabricated composites were cut from the cast ingot for microstructural examinations. Specimens were ground under water on a rotating disc using SiC abrasive discs of increasing finesse up to 1200 grit. Then they were polished using 10 μm alumina paste and 3 μm diamond paste. Microstructural examinations were conducted using both optical and scanning electron microscopes (SEM). Microstructural examination was performed in the unetched condition. The porosity of the MMNCs was measured using the typical Archimedes (water displacement) method.

The electrical measurements of the A356 monolithic alloy and the A356/Al_2O_3 MMNCs were measured using SIGMASCOPE SMP10 apparatus made by Helmut Fischer GmbH + Co.KG, Germany. The apparatus can measure the electrical conductivity of all non-magnetic metals and even stainless steel, etc. Samples from the MMNCs and the monolithic alloy having a cylindrical shape of 20 mm diameter and 10 mm length were cut from the cast and polished from the two end faces before electrical conductivity measurements. The electrical conductivity measurements were performed according to ASTM E-1004. The apparatus measures the electrical conductivity using the eddy current method.

The thermal conductivity of the MMNCs was measured using the apparatus shown in **Figure 1**. The apparatus has been specially designed for the determination of thermal conductivity for both good conductors and thin specimens of insulants. The apparatus consists of a self-clamping specimen stack assembly with electrically heated source, calorimeter base, Dewar vessel enclosure to ensure negligible loss of heat, and constant head cooling water supply tank. A multipoint thermocouple switch is mounted on the MMNCs specimen and two mercury and glass thermometers are provided for water inlet and outlet temperature readings as shown in **Figure 2**.

Three NiCr/NiAl thermocouples are fitted and connections are provided for a suitable potentiometer instrument to give accurate temperature readings. The specimens have cylindrical shape of about 10 mm diameter and 20 mm length. The end faces of these specimens are very carefully prepared by grinding and lapping operations. Two small holes were drilled in each specimen for insertion of the thermocouples. Heat was applied to the top of the stack of specimens by contact with the thermostatically protected heater block, and is collected at the base of the stack by contact with a water cooled calorimeter. The heat transmitted through the specimens can thus be

Figure 1. A photograph of the apparatus used to measure the thermal conductivity of the nanocomposites.

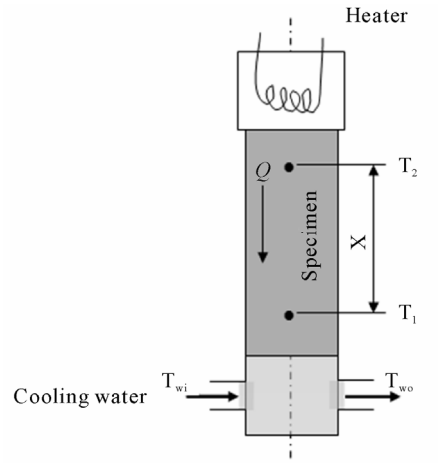

Figure 2. A schematic drawing shows the specimen, the positions of the thermocouples and the heating and cooling methods of the specimen.

calculated from a measurement of water flow and temperature rise of the water. Heat losses by radiation and conduction from the heater block other than from contact with the specimen were neglected, since measurement is made of heat collected from the samples rather than heat delivered to them. A steady flow of cooling water is maintained at the end away from the heating block and it leaves at the end nearer to it. Thermometers T_{wi} and T_{wo} are provided to measure the temperatures of the inlet and outlet water, respectively. Two holes of 1.5 mm diameter are drilled in the specimen rod and thermocouples are inserted in these holes to measure the temperatures T_1 and T_2 of the rod at these places. The temperatures of the two thermometers and the two thermocouples rise initially and ultimately become constant when the steady state is reached. The water coming out of the apparatus is collected in a beaker for a fixed time measured by a stopwatch and the flow rate of water is determined by timing the collection of 100 cm^3 per second sample of water. The cross-section area of the rod is calculated by measuring its diameter and the distance between the holes in the rod was measured.

It is assumed that the cross-sectional area normal to the flow of heat transfer is constant and the periphery is insulated due to the use of Dewar vessel enclosure to ensure negligible loss of heat. The heat transfer through the specimen rod is governed by Fourier's Law:

$$Q = -kA\frac{\mathrm{d}T}{\mathrm{d}x} \tag{1}$$

where Q is the rate of heat transfer in the x-direction, k is the thermal conductivity of the specimen material, A is the cross-sectional area of the specimen normal to the x-direction, and $\mathrm{d}T/\mathrm{d}x$ is the temperature gradient in the x-direction. At steady state condition the temperature of the specimen does not change with time at any point and the heat conducted along the specimen must go into the flowing water. The heat taken by the water was calculated using the following equation:

$$Q = mc_p\left(T_{wo} - T_{wi}\right) \tag{2}$$

where m is the mass flow rate of cooling water, C_p is the specific heat of water, and T_{wo}, T_{wi} are the cooling water outlet and inlet temperatures, respectively. By applying a thermal balancing hence, the same rate of heat transfer Q is used in Equation (1) and (2). Thus,

$$k = \frac{mc_p\left(T_{wo} - T_{wi}\right)x}{A\left(T_2 - T_1\right)} \tag{3}$$

The thermal conductivity measurement depends on the measurement of the heat flux Q and temperature difference ($T_2 - T_1$). The axial flow method has been long established and has produced some of the most consistent and highest accuracy results. The present measurement focused mainly on reduction of radial heat losses in the axial heat flow developed through the specimen from the electrical heater mounted at one end.

3. Results and Discussion

3.1. Microstructural Observations

Figure 3 shows typical micrographs for the microstructure of the monolithic A356 alloy as well as the fabricated A356/Al_2O_3 MMNCs after heat treatment. It is clear from **Figure 3(a)** that the structure of the monolithic A356 Al alloy consists of primary α phase (white regions) and Al-Si eutectic structure (darker regions). Fine needle-like primary Si particulates were distributed along the boundaries of the α-Al dendrites. **Figures 3(b)** and **3(c)** show micrographs of A356/Al_2O_3 MMNCs con-

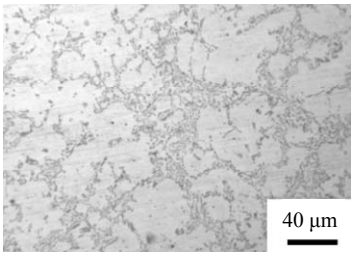

(a)

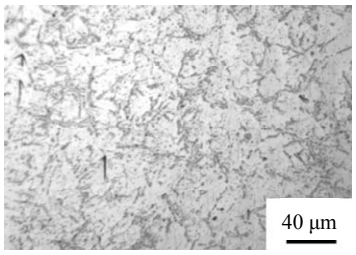

(b)

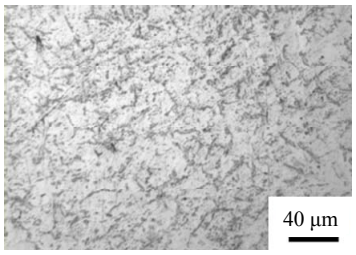

(c)

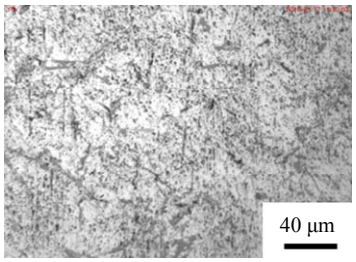

(d)

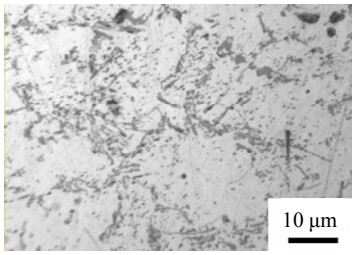

(e)

Figure 3. Optical micrographs for (a) A356 monolithic aluminum alloy; (b) A356/3 vol% Al_2O_3 (60 nm) nanocomposites; (c) A356/3 vol% Al_2O_3 (200 nm) nanocomposites; (d) A356/5 vol% Al_2O_3 (200 nm); (e) A356/5 vol% Al_2O_3 (200 nm) nanocomposites.

taining 3 vol% of Al_2O_3 nanoparticles having 60 and 200 nm, respectively. Clusters of Al_2O_3 nanoparticles in the microstructure of the A356/Al_2O_3 MMNCs were observed. **Figure 3(d)** shows high magnification optical micrograph of Al_2O_3/5 vol% (200 nm) MMNCs. It is clear that clusters of nanoparticles clusters are located inside the α-grains as well as near the eutectic structure. **Figure 4(a)** shows high magnification SEM micrograph of the 5 vol% Al_2O_3 nanoparticles (200 nm) showing that nanoparticles are agglomerating near the Si particles of the eutectic structure. The XRD analysis for the nanoparticles is shown in **Figure 4(b)**. Increasing the volume fraction of the Al_2O_3 nanoparticles dispersed inside the A356 alloy increases the agglomeration percent. The

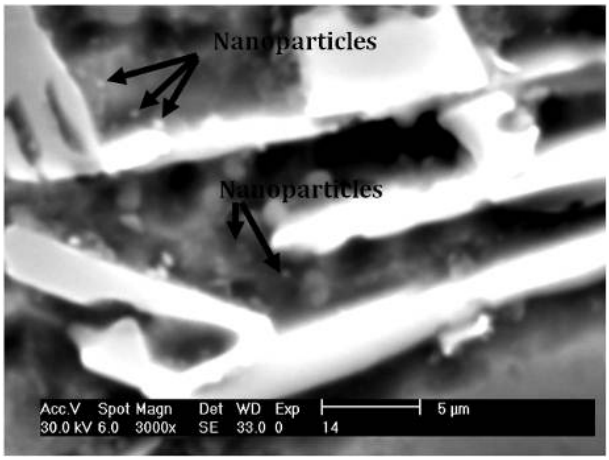

(a)

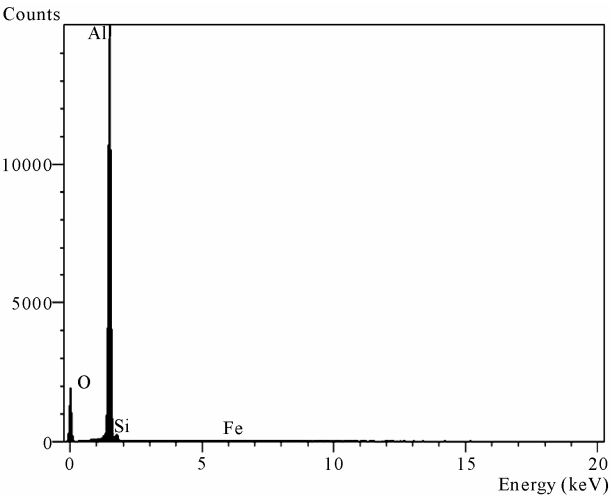

(b)

Figure 4. (a) High magnification SEM micrograph of the 5 vol% Al_2O_3 nanoparticulates (200 nm) showing that nanoparticulates are agglomerating near the Si particles of the eutectic structure; (b) XRD analysis for the particles shown in (a).

MMNCs containing 5 vol% of Al_2O_3 nanoparticles exhibited the highest agglomeration percent when compared with those containing 1 and 3 vol%.

Porosity measurements indicted that the MMNCs have porosity content lower than 2 vol%. Such low porosity content is attributed to the squeezing process that was carried out during the solidification of the MMNCs. In cast MMCs, there are several sources of gases. The occurrence of porosity can be attributed variously to the amount of hydrogen gas present in the melt, the oxide film on the surface of the melt that can be drawn into it at any stage of stirring and the gas being draw into the melt by certain stirring methods. Vigorously stirred melt or vortex tends to entrap gas and draw it into the melt. Increasing the stirring time allows more gases to be entered into the melt and hence reduce the mechanical properties.

The amount of liquid inside the semi-solid slurry increases with increasing the temperature which on the other hand reduces the viscosity of the solid/ liquid slurry. Nanoparticle distribution in the A356 Al matrix alloy during the squeezing process depends greatly on the viscosity of the slurry and also on the characteristics of the reinforcement particles themselves, which influence the effectiveness of squeezing in to break up agglomerates and distribute particles. When the amount of liquid inside the slurry is large enough, the particles can be rolled or slid over each other and thus breaking up agglomerations and helping the redistribution of nanoparticles and improving the microstructure.

3.2. The Thermal Conductivity of MMNCs

Figure 5 shows the variation of the thermal conductivity against the time for different MMNCs specimens having different volume fractions and sizes of Al_2O_3 nanoparticles. The figure shows that there is a significant variation of the thermal conductivity during the first few minutes and it approaches to a relatively constant value after 120 minutes or two hours (Steady state condition). The A356/5 vol% contains Al_2O_3 nanoparticles of 200 nm and 60 nm exhibited the maximum and the minimum values of thermal conductivity of 213 and 105 W/m.K, respectively. The present experimental measurements show a signifycant difference in the value of the average thermal conductivity for different A356/Al_2O_3 MMNCs. The steady state technique and the axial flow method are satisfactory methods for measuring the thermal conductivity of MMNCs.

The variation of the thermal conductivity of the A356/Al_2O_3 MMNCs with the volume fraction of the nanoparticles at several nanoparticles sizes is shown in **Figure 6**. The thermal conductivities of the A356/Al_2O_3 MMNCs showed disturbing results. It is suggested that the clustering of the Al_2O_3 nanoparticles is the reason of such

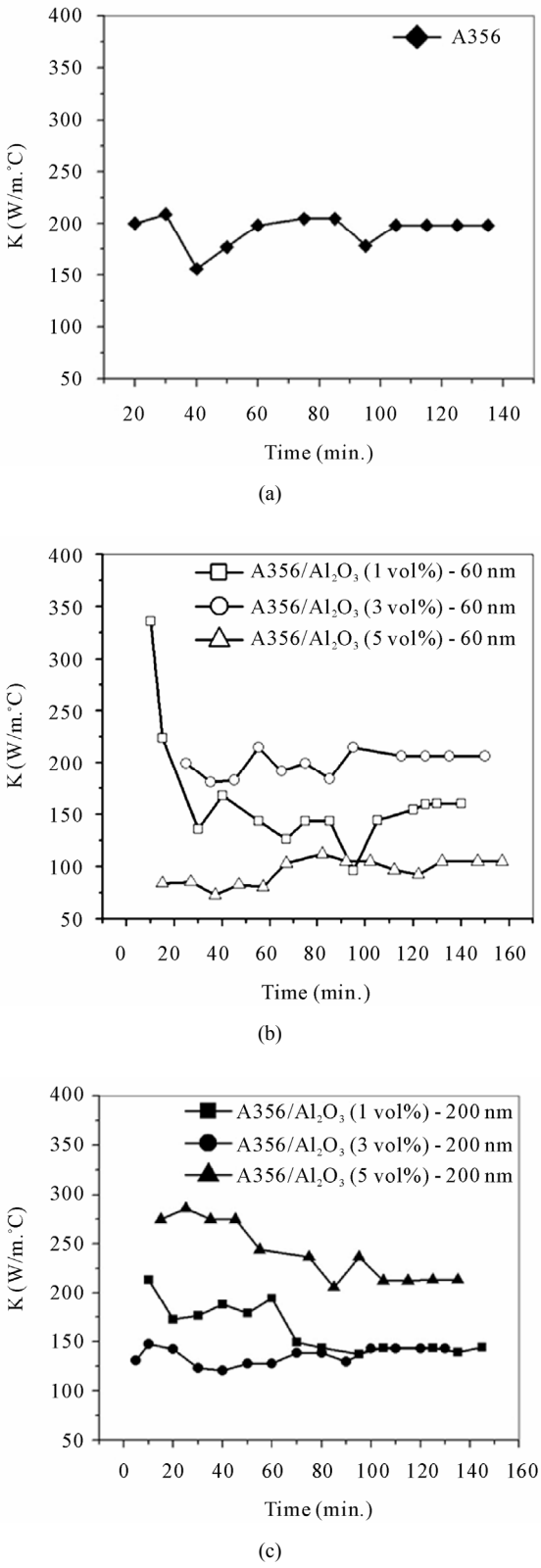

Figure 5. Variation of average thermal conductivity with the time for (a) the A356 monolithic alloys; (b) A356/Al_2O_3 (60 nm) MMNCs and (c) A356/Al_2O_3 (200 nm) MMNCs.

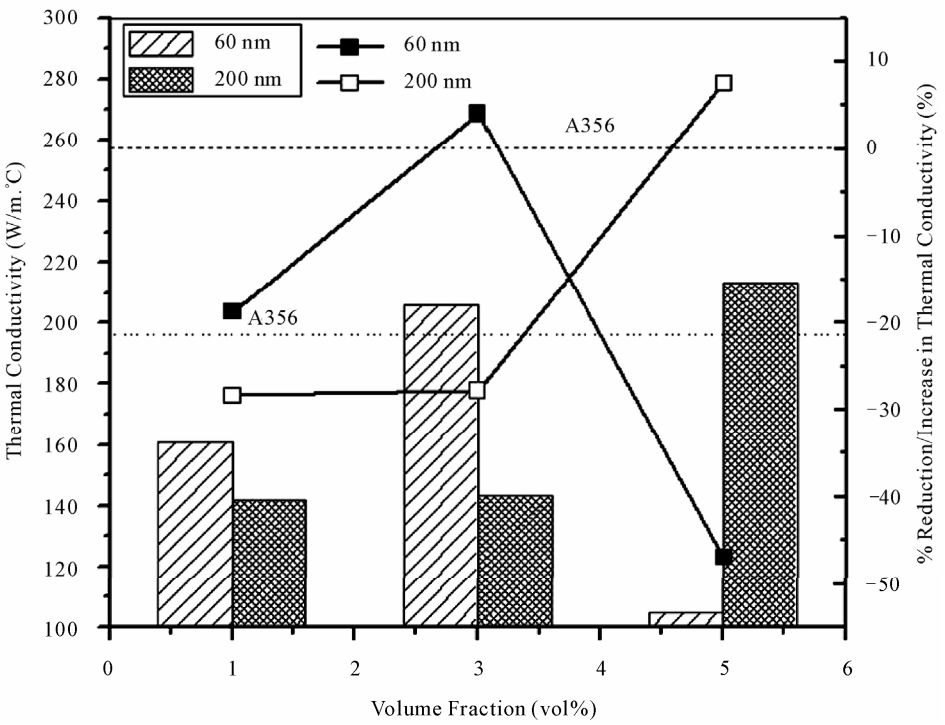

Figure 6. The average thermal conductivity of the A356/Al_2O_3 MMNCs.

results. Generally, the Al_2O_3 nanoparticles addition decreased the thermal conductivity of the MMNCs when compared with the A356 monolithic alloy. The MMNCs containing up to 3% of 60 nm Al_2O_3 nanoparticles showed better thermal conductivities than those containing 200 nm nanoparticles. Only MMNCs containing 3%-60 nm and 5%-200 nm of Al_2O_3 nanoparticles showed practically the same thermal conductivity of A356. The reducetion of the thermal conductivity of the MMNCs due to the addition of the Al_2O_3 nanoparticles may attribute to the insulating nature of the Al_2O_3 nanoparticles itself and the increase of the porosity content with increasing the volume fraction of the nanoparticles. **Figure 6** shows also the percent of reduction/increase of the thermal conductivity of A356 due to the dispersion of Al_2O_3 nanoparticles having several sizes and volume fractions. The maximum percentage of reduction of thermal conductivity was about 47% for MMNCs containing 5 vol% of 60 nm particulates.

The reduction of the thermal conductivity due to the addition of ceramic nanoparticles was also reported by Ke Chu *et al.* [11]. They reported that the addition of carbon nanotubes (CNTs) showed no enhancement in overall thermal conductivity of the Cu composites due to the interface thermal resistance associated with the low phase contrast of CNT to copper and the random tube orientation. Besides, the composite containing 15 vol% CNTs led to a rather low thermal conductivity due possibly to the combined effect of unfavourable factors induced by the presence of CNT clusters, *i.e.* large porosity and lower effective conductivity of CNT clusters themselves.

The thermal conductivity of the conventional aluminium based MMCs was investigated by many workers [12,13]. It has been found that the thermal conductivity of MMCs is mainly governed by the conductivity of the individual phases, their volume fraction and shape, and also by the size of the inclusion phase due to a finite metal/ceramic interface thermal resistance. Beside these factors, the results obtained from the current work showed that the agglomeration % of the particulates has a significant influence on the thermal conductivity of the MMCs. Increasing the volume fraction of the particulates increases the amount of agglomeration % of the particles which can lead to disturbing results of the average thermal conductivity of the MMCs. Particles free zones have higher thermal conductivity than the particles clustered zones. Another important factor that plays an important role on the thermal conductivity of the MMCs is the fabrication technique and its processing conditions. The casting techniques have several advantages than other fabrication techniques such as powder metallurgy. These advantages include lower cost and the capability of production of large components. However, MMCs cast components suffer from several defects such as particles segregation and high porosity content. The choice of the

proper process parameters of the casting technique has a significant effect in reduction, but not elimination, of the particles segregation and porosity content. Squeezing the MMNCs during solidification helped in reduction of the porosity content of the MMNCs, however, it did not reduce the agglomeration % of the particles. The reduction of the agglomeration % of the particles can be achieved by the proper selection of the rheocasting process parameters which was the previous stage before the squeezeing process. The rheocasting process parameters include; the stirring speed; the shape, position and size of the stirrer; the stirring temperature; the stirring duration and pouring technique.

3.3. Electrical Conductivity of MMNCs

Figure 7 shows the variation of the electrical conductivity of the A356/Al_2O_3 MMNCs, in MS/m, with the volume fraction of the Al_2O_3 nanoparticles. The results revealed that the MMNCs showed lower electrical conductivities when compared with the A356 base alloy. Increasing the volume fraction reduces the electrical conductivity of the MMNCs. Moreover, the increasing the size of the nanoparticles from 60 to 200 nm reduced significantly the electrical conductivity of the MMNCs. The maximum reduction percent in the conductivity, with respect to the A356 monolithic alloy, was about 38% and exhibited by A356/Al_2O_3 MMNCs containing 5 vol% of nanoparticles having 200 nm.

The reduction of the electrical conductivity of the A356 due to the addition of the Al_2O_3 nanoparticles may be attributed to the clustering of the nanoparticles which are in fact insulations sites that reduce the electrical conductivity. Moreover, it has been observed that the nanoparticles are positioned and clustered at the grain boundaries of Al grains and decrease the electrical conductivity. The reduction of the electrical conductivity due to the addition of ceramic nanoparticles noticed in the current work has been observed also by Sheikh *et al.* [10]. In their work, carbon nanotubes were (CNT) added to pure copper and MMNCs were fabricated using powder metallurgy. The results revealed that increasing CNT contents in the Cu composites decreases the electrical conductivity. In contrast, *El-Mahallawi et al.* [14] reported that introducing Al_2O_3 nanoparticles to A356 alloy within the range 1 vol% tends to yield the alloy of highest electrical conductivity of the MMNCs. The morphology, and size of the eutectic silicon is believed to have an effect on the electrical conductivity also and any improvement on the eutectic morphology is believed to induce a significant effect on the electrical conductivity of the A356 alloy [14]. The significant effect induced on cast alloys by adding Al_2O_3 particulates has been discussed and reported recently by some researchers. Generally, the electrical conductivity of the MMCs is mainly decided by the conductivity of the matrix alloy as well as the shape, size and volume fraction of hard ceramic alumina particles [15].

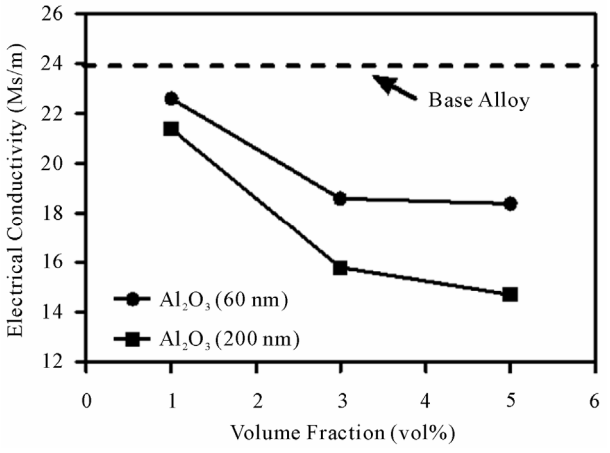

Figure 7. Variation of the electrical conductivity of the A356/Al_2O_3 MMNCs with the volume fraction of the Al_2O_3 nanoparticles.

4. Conclusions

Based on the results obtained from the current work, the following conclusions are drawn:

1) The A356 monolithic alloy exhibited better thermal conductivity than the MMNCs. The A356/Al_2O_3 MMNCs containing up to 3% of 60 nm Al_2O_3 nanoparticles showed better thermal conductivities than the MMNCs containing 200 nm nanoparticles.

2) The A356/Al_2O_3 MMNCs showed lower electrical conductivities when compared with the A356 base alloy. Increasing the volume fraction of the Al_2O_3 nanoparticles reduces the electrical conductivity of the MMNCs. Moreover, increasing the size of the Al_2O_3 nanoparticles from 60 to 200 nm reduced significantly the electrical conductivity of the MMNCs.

3) The maximum reduction percent in the thermal and electrical conductivities, according to the A356 monolithic alloy, were about 47% and 38%, respectively. These percentages were exhibited by A356/Al_2O_3 MMNCs containing 5 vol% of nanoparticles having 60 and 200 nm, respectively.

5. Acknowledgements

This work is supported by the King Abdel-Aziz City of Science and Technology (KACST) through the Science and Technology Center at King Khalid University (KKU), Fund (NAN 08-172-7). The authors thank both KACST and KKU for their financial support. Special Thanks to Prof. Dr. Saeed Saber, Vice President of KKU, Dr. Ahmed Taher, Dean of the Scientific Research at

KKU, and Dr. Khaled Al-Zailaie**,** Dean of the faculty of engineering at KKU, for their support.

REFERENCES

[1] ASM Handbook, "Composites," *ASM International*, Vol. 21, 2001.

[2] N. Chawla and K. K. Chawla, "Metal Matrix Composites," Springer Science and Business Media Inc., Berlin, 2006,

[3] B. Cantor, F. P. E. Dunne and I. C. Stone, "Metal and Ceramic Matrix Composites," Taylor & Francis, New York, 2003.

[4] J. Hashim, L. Looney and M. S. J. Hashmi, "Metal Matrix Composites: Production by the Stir Casting Method," *Journal of Materials Processing Technology*, Vol. 92-93, 1999, pp. 1-7. doi:10.1016/S0924-0136(99)00118-1

[5] K. Miwa and T. Ohashi, "Preparation of Fine SiC Particle Reinforced Al. Alloy Composites by Compocasting Process," *Proceedings of the 5th Japan-U.S. Conference on Composite Materials*, Tama City, Tokyo, 24-27 June 1990, pp. 355-362.

[6] T. S. Mahmoud, F. H. Mahmoud, H. Zakaria and T. A. Khalifa, "Effect of Squeezing on Porosity and Wear Behaviour of Partially Remelted A319/20 vol% SiC_p MMCs," *Proceedings of the Institution of Mechanical Engineers, Part C*: *Journal of Mechanical Engineering Science*, Vol. 222, No. C3, 2008, pp. 295-303. doi:10.1243/09544062JMES803

[7] F. R. Rahmani and F. Akhlaghi, "Effect of Extrusion Temperature on the Microstructure and Porosity of A356-SiC_p Composites," *Journal of Materials Processing Technology*, Vol. 187-188, 2007, pp. 433-436. doi:10.1016/j.jmatprotec.2006.11.077

[8] A. Ansary Yar, M. Montazerian, H. Abdizadeh and H. R. Baharvandi, "Microstructure and Mechanical Properties of Aluminum Alloy Matrix Composite Reinforced with Nano-Particle MgO," *Journal of Alloys and Compounds*, Vol. 484, No. 1-2, 2009, pp. 400-404. doi:10.1016/j.jallcom.2009.04.117

[9] J. Lan, Y. Yang and X. C. Li, "Microstructure and Microhardness of SiC Nanoparticles Reinforced Magnesium Composites Fabricated by Ultrasonic Method," *Materials Science and Engineering A*, Vol. 386, No. 1-2, 2004, pp. 284-290.

[10] S. M. Uddin, T. Mahmud, C. Wolf, C. Glanz, I. Kolaric, C. Volkmer, H. Höller, U. Wienecke, S. Roth and H.-J. Fecht, "Effect of Size and Shape of Metal Particles to Improve Hardness and Electrical Properties of Carbon Nanotube Reinforced Copper and Copper Alloy Composites," *Composites Science and Technology*, Vol. 70, No. 16, 2010, pp. 2253-2257.

[11] K. Chu, Q. Y. Wu, C. C. Jia, X. B. Liang, J. H. Nie, W. H. Tian, G. S. Gai and H. Guo, "Fabrication and Effective Thermal Conductivity of Multi-Walled Carbon Nanotubes Reinforced Cu Matrix Composites for Heat Sink Applications," *Composites Science and Technology*, Vol. 70, No. 2, 2010, pp. 298-304.

[12] S. K. Chaudhury, A. K. Singh, C. S. Sivaramakrishnan and S. C. Panigrahi, "Effect of Processing Parameters on Physical Properties of Spray Formed and Stir Cast Al-2Mg-TiO_2 Composites," *Materials Science and Engineering A*, Vol. 393, No. 1-2, 2005, pp. 196-203. doi:10.1016/j.msea.2004.10.010

[13] M. Molina, J. Narciso, L. Weber, A. Mortensen and E. Louis, "Thermal Conductivity of Al–SiC Composites with Monomodal and Bimodal Particle Size Distribution," *Materials Science and Engineering A*, Vol. 480, No. 1-2, 2008, pp. 483-488. doi:10.1016/j.msea.2007.07.026

[14] I. S. El-Mahallawi, K. Eigenfield, F. Kouta, A. Hussein, T. S. Mahmoud, R. M. Ragaie, A. Y. Shash and W. Abou-Al-Hassan, "Synthesis and Characterization of New Cast A356/(Al_2O_3)P Metal Matrix Nano-Composites," *ASME*, *Proceeding of the* 2*nd Multifunctional Nanocomposites & Nanomaterials*, *International Conference & Exhibition*, Organized by the American University in Cairo—AUC, in Collaboration with Cairo University, Sharm El Sheikh, Egypt, 11-13 January 2008.

[15] L. Weber, J. Dorn and A. Mortensen, "On the Electrical Conductivity of Metal Matrix Composites Containing High Volume Fractions of Non-Conducting Inclusions," *Acta Materialia*, Vol. 51, No. 11, 2003, pp. 3199-3211. doi:10.1016/S1359-6454(03)00141-1

